JMEPEG (2009) 18:102–105
DOI: 10.1007/s11665-008-9266-9
©ASM International
1059-9495/$19.00

Microstructural Analysis of $TiAl_xN_yO_z$ Coatings Fabricated by DC Reactive Sputtering

L. García-González, J. Hernández-Torres, N. Flores-Ramírez, J. Martínez-Castillo, P.J. García-Ramírez, J. Muñoz-Saldaña, and F.J. Espinoza-Beltrán

(Submitted October 10, 2007; in revised form May 12, 2008)

$TiAl_xN_yO_z$ coatings were prepared by DC reactive sputtering on AISI D2 tool steel substrates, using a target of Ti-Al-O fabricated from a mixture of powders of Ti (22.60 wt.%), Al (24.77 wt.%), and O (52.63 wt.%). The coatings were deposited on substrates at room temperature in a reactive atmosphere of nitrogen and argon under a pressure of 8.5×10^{-3} mbar. X-ray diffraction, electron dispersive spectroscopy, Raman scattering, and nanoindentation techniques were employed to investigate the coatings. The results show that the increment in the nitrogen flow affects the structure and the mechanical properties of the coatings. The sample with the lowest nitrogen flow presented the highest hardness (10.5 GPa) and the Young's modulus (179.5 GPa). The hardness of the coatings $TiAl_xN_yO_z$ as a function of crystalline grain size shows a behavior consistent with the Hall–Petch relation.

Keywords DC reactive sputtering, microstructure, $TiAl_xN_yO_z$ coatings, Warren–Aberbach method

1. Introduction

$TiAl_xN_yO_z$ coatings systems have good mechanical properties, low densities, and good oxidation resistance. These exceptional properties make $TiAl_xN_yO_z$ coatings very important technological materials for high-temperature applications (Ref 1) as well as candidates for diffusion barriers for metallization (Ref 2-5). $TiAl_xN_yO_z$ coatings are most commonly deposited by reactive magnetron sputtering, often using a TiAl target and varying the oxygen content (Ref 2-5). In these works, the reported values of hardness were around 35 GPa. Although the mechanical properties of $TiAl_xN_yO_z$ coatings are documented satisfactorily, relatively few investigations have been carried out to study the correlation among crystalline grain size distribution, intrinsic stress, and hardness.

In the present work, the influences of nitrogen flux on microstructures and mechanical properties of $TiAl_xN_yO_z$ coatings are studied. The hardness of the coatings is analyzed in correlation with the grain size for each sample.

L. García-González, J. Martínez-Castillo, and **P.J. García-Ramírez**, Centro de Investigación en Micro y Nanotecnología, Universidad Veracruzana, Boca del Río, Veracruz 94292, México; **J. Hernández-Torres**, Universidad del Papaloapan, Campus Loma Bonita, Loma Bonita, Oaxaca 68400, México; **N. Flores-Ramírez**, Faculty of Wood Engineering and Technology, Universidad Michoacana de San Nicolás de Hidalgo, Morelia, Michoacán 58000, México; and **J. Muñoz-Saldaña** and **F.J. Espinoza-Beltrán**, Centro de Investigación y de Estudios Avanzados del IPN, Unidad Querétaro, Qro 76230, México. Contact e-mail: leagarcia@uv.mx.

2. Experimental

$TiAl_xN_yO_z$ coatings were deposited on AISI D2 tool steel substrates by DC reactive sputtering technique (Intercovamex—sputtering device V3) using a target of Ti-Al-O fabricated from a mixture of powders of Ti (22.60 wt.%), Al (24.77 wt.%), and O (52.63 wt.%). The residual vacuum in the chamber was 1×10^{-6} mbar, with a maximum vacuum of 8.5×10^{-3} mbar and with a power of 200 W for 2 h. The flow rate of argon was maintained constant at 25 sccm for all the coatings. Sets of coatings were identified as M1_2.5, M2_5.0, M3_10.0, and M4_15.0, for nitrogen flow rates 2.5, 5.0, 10.0, and 15.0 sccm, respectively.

The structure of the $TiAl_xN_yO_z$ coatings was analyzed by XRD in a RIGAKU diffractometer, model DMAX/1200, working with CuK_α radiation (1.5406 Å). Vibrational modes of the coatings were studied by Raman scattering spectroscopy (RSS), where the coatings were excited with a helio-neon laser of 632.8 nm with a power of 20 mW, using a time of integration of 25 s over an area of 2 μm in diameter. Chemical composition of these coatings was determined by energy dispersive X-ray spectroscopy (EDS) using an environmental scanning electron microscopy (PHILIPS XL30 ESEM). All nanoindentation tests (Hysitron Ubi1) were performed in load control mode with a Berkovich tip. For each sample several series of ten indents were made and the results were averaged. For each indent 9.0 mN maximum load was used with the increasing steps of 1.0 mN.

3. Results and Discussion

The X-ray diffraction patterns for all coatings fabricated with nitrogen flux varied between 2.5 and 15 sccm are shown in Fig. 1. The patterns show a mixture of three crystalline phases, fcc-Ti_3AlN (JADE-PDF—card # 37-1140), hex-$Ti_3Al_2N_2$ (JADE-PDF—card # 37-1141) y ortho-$Ti_{2.46}Al_{0.54}N_{0.28}O_{4.58}$

(JADE-PDF—card # 37-42-1279). In this figure it is observed that the relationship of the diffraction peak intensities does not follow the powder intensities relation. These results are in accord with the report by Kim and Alford (Ref 2), who found that the $TiAl_xN_yO_z$ system is a phase mixture of Ti-Al-N and Ti-Al-N-O. Alternate changes in the preferred orientations are observed as the nitrogen flux increases, until the sample M4_15.0 is reached, which presents peaks with low intensity. The pattern of all samples in Fig. 1 was analyzed using the Warren–Averbach method (Ref 6), obtaining a crystallite size in the range of 6.1-10.8 nm, which is presented in Fig. 2. With this method, the X-ray diffraction pattern peaks are corrected for the broadening of the diffraction lines, Lorentz dispersion, and diffraction due to the Cu-$K_{\alpha 2}$ line and then submitted to Fourier analysis. The Warren–Averbach method assumes that peak widening is due to the size distribution of the crystalline grains and to deformations due to internal stress in the lattice. The Pearson VII function was used for the line adjustments in the X-ray diffraction peaks. The advantage of using the Warren–Averbach analysis to obtain average grain size is that it proves more consistent grain size values, even for samples with XRD patterns with superimposed peaks.

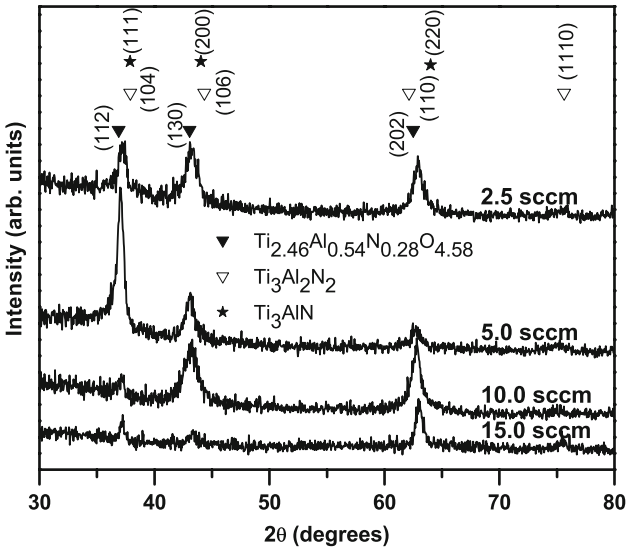

Fig. 1 XRD patterns of M1_2.5, M2_5.0, M3_10.0, and M4_15.0 coatings

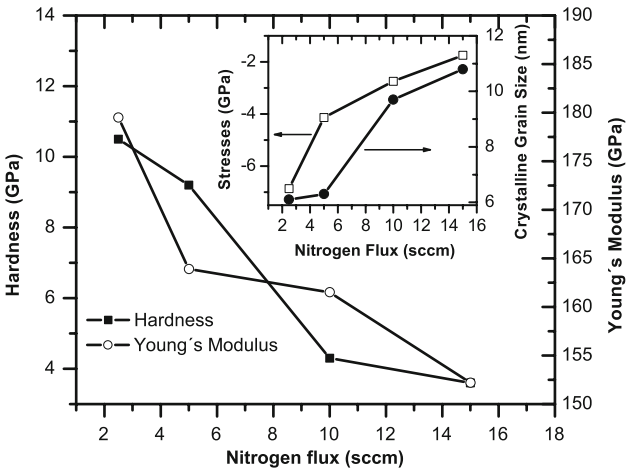

Fig. 2 Effects of nitrogen flux on structure and mechanicals properties of M1_2.5, M2_5.0, M3_10.0, and M4_15.0 coatings

Figure 2 shows the hardness and Young's modulus data for all samples. As can be observed there is a similar behavior in hardness and Young's modulus with the increase in the nitrogen flux for all the samples. A maximum in indentation hardness and Young's modulus, with 10.5 and 179.5 GPa, respectively, is observed for the coating deposited at a nitrogen flux of 2.5 sccm. The main cause for this hardness increase is the lattice distortion, and consequent reduction in dislocations motion, which occurs in order to accommodate the nitrogen atoms in the titanium lattice (Ref 7). In the same way, this can be understood in light of its smaller crystalline grain size. On the other hand, the coating fabricated at a nitrogen flux of 15 sccm exhibits a lower hardness and Young's modulus of 3.6 and 152.2 GPa, respectively. The nitrogen flow is a parameter that significantly can affect the discharge conditions in the sputerring process and therefore, the overall chemical composition of the coatings, this is, their stoichiometric composition. The inset in Fig. 2 shows the plot of intrinsic stress and crystalline grain size as a function of the nitrogen flux. The intrinsic stress was obtained using the Stoney formula (Ref 8):

$$\sigma_s = -\frac{E}{\mu}\frac{d - d_0}{d_0} \qquad \text{(Eq 1)}$$

This considers the difference in the 2θ position of the diffraction peaks of the sample under investigation, with respect to those of the non-stressed reference. In the Stoney formula, E is the Young's modulus, μ the Poisson's ratio, d_0 the strain-free reference lattice spacing, and d is the lattice spacing obtained from the diffraction pattern of the sample under investigation. The values obtained correspond to compressive stress and are in the range from approximately 1.75 to 6.86 GPa. A maximum compressive stress (about −6.86 GPa) for the coating of highest hardness is obtained.

According to these results, harder $TiAl_xN_yO_z$ coatings have smaller crystalline grain size and larger intrinsic stresses. In most materials, including metals and brittle ceramics, hardness increases with decreasing grain size. This behavior is described by the Hall–Petch relationship (Ref 9, 10). However, it has been reported that this relation does not work properly for some materials (Ref 11), where a softening ("inverse Hall–Petch effect") with decreasing grain size is observed. Nevertheless, in our case it was found that the hardness of the $TiAl_xN_yO_z$ coatings follows a behavior similar to that predicted by the Hall–Petch relation. Figure 3 shows the fitting of the experimental data, H, to the Hall–Petch relation (Ref 9, 10)

$$H = H_0 + k/\sqrt{L} \qquad \text{(Eq 2)}$$

where H_0 (= −16.761 GPa) and k (= 66.24 GPa/nm$^{-1/2}$) are the fitting parameters. The increase of hardness with the grain size decrease is well described by the Hall–Petch relation, and it is explained by the pile up of dislocations on grain boundaries (Ref 12). For $TiAl_xN_yO_z$ crystalline grain size approximately 6 nm and larger, the dislocations into the crystals are scarce, so that a limited grain boundary sliding determines the material deformation and hardness. The behavior of nanocrystalline materials, with a grain size of about 10 nm or less, is determined mainly by processes in boundary regions because the number of atoms in the grains is comparable to or smaller

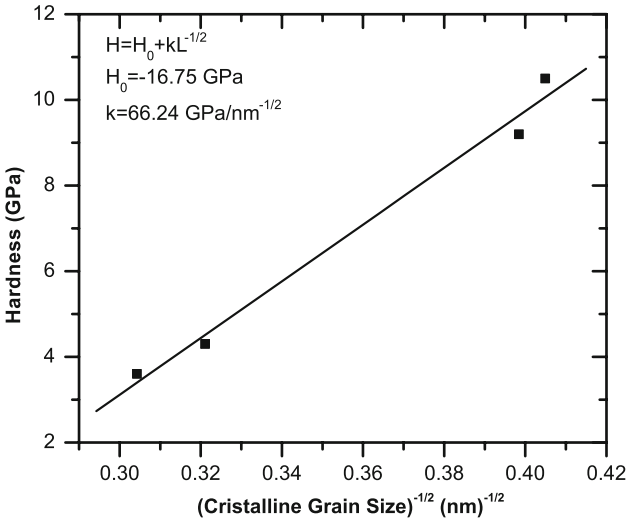

Fig. 3 Hardness of $TiAl_xN_yO_z$ coatings as a function of square root of grain size, and the fitting of the experimental data to the Hall–Petch relation

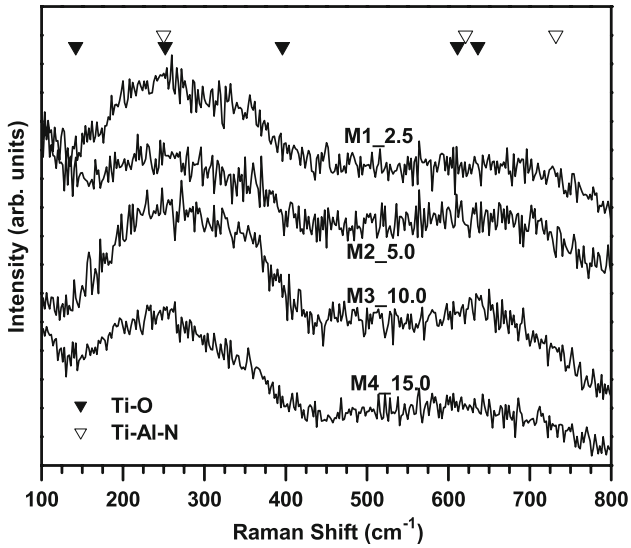

Fig. 4 Raman scattering spectra for M1_2.5, M2_5.0, M3_10.0, and M4_15.0 coatings

than that in the boundary regions. Under these conditions dislocations do not exist (Ref 13), because grain boundaries prevent their formation, and the boundary regions play a decisive role in the material deformation. A new deformation mechanism, called grain boundary sliding, replaces the dislocation activity which is the dominant deformation process in conventional materials (Ref 14).

The results obtained by EDS reveal that the reactive sputtered coatings contain the following atomic compositions: M1_2.5 (Ti: 1; Al: 0.82; N: 1.10; and O: 1.39), M2_5.0 (Ti: 1; Al: 0.74; N: 1.29; and O: 1.42), M3_10.0 (Ti: 1; Al: 0.77; N: 1.48; and O: 1.48) and M4_15.0 (Ti: 1; Al: 0.77; N: 1.57; and O: 1.25). These results indicate that small variations exist in Al and O, as the nitrogen flow is increased.

Nanocrystalline Ti-O and Ti-Al-N were detected by RSS in all coatings even though the detection of Ti-O and Ti-Al-N is difficult. Figure 4 shows the Raman scattering spectra for all coatings, with the Ti-O and Ti-Al-N spectral line indicating positions shown by vertical lines. All the coatings show flat spectra due to deviations from stoichiometry. The Raman shift line broadening is observed in the range between 150 and 350 cm^{-1}, being obtained a maximum for all the samples in 250 cm^{-1}, which corresponds to the pick of more intensity reported in the literature for the TiAlN (Ref 15). In this same range is observed the pick of 142 cm^{-1}, corresponding to the pick of more intensity for the anatasa (Ref 16). This behavior is shown for all the samples, corroborating this way the results obtained by X-ray diffraction.

4. Conclusion

$TiAl_xN_yO_z$ coatings can be prepared in the gaseous mixture of Ar and N_2 by DC reactive sputtering using a target of Ti-Al-O fabricated from a mixture of powders of Ti (22.60 wt.%), Al (24.77 wt.%), and O (52.63 wt.%). The Warren–Averbach method was used to analyze the experimental X-ray diffraction lines. It was found that the crystalline grain size as well as the coatings hardness strongly depends on the nitrogen flow. An increase in nitrogen flow increases the surface mobility of the atoms of the coating, obtaining larger crystalline grains and intrinsic stresses. It is observed that the intrinsic stress and hardness have a behavior proportional to the inverse of square root of crystalline grain size, similar to the Hall–Petch relation. The increase of hardness with a decrease in grain size has been explained on the basis of pile up of dislocations on the grain boundaries. Finally, the reactivity in an Ar-N_2 environment is strongly governed by the thermochemical behavior of each constituent in the respective Ti/Al-N/O system, as the nitrogen gas tends to react more with Ti than with Al, since the free energy of formation of TiN is lower than that of AlN, obtaining this way different crystalline grain size and consequently different values of hardness.

Acknowledgments

This work was supported by CONACYT under Projects 66812 and 56642. Participation of María del Carmen Mendoza Ruiz, Teresa Carrano Guerra, Pedro García Jiménez, Martín Adelaido Hernández Landaverde, José Eleazar Urbina Álvarez, and Raúl Juárez Aguirre is acknowledged.

References

1. H.J. Seifert, A. Kussmaul, and F. Aldinger, Phase Equilibria and Diffusion Paths in the Ti–Al–O–N System, *J. Alloy Compd.*, 2001, **317–318**, p 19–25
2. H.C. Kim and T.L. Alford, Investigation on Diffusion Barrier Properties of Reactive Sputter Deposited $TiAl_xN_yO_z$ Thin Films for Cu Metallization, *Thin Solid Films*, 2005, **449**(1–2), p 6–11
3. Y. Liu, Y. Dong, W. Zhao, and G. Li, Microstructure and Mechanical Properties of (Al, Ti)(O, N) Coatings Prepared by Reactive Sputtering, *Int. J. Refract. Met. H*, 2007, **25**(3), p 271–274
4. F. Mei, Y. Dong, Y. Li, and G. Li, Microstructure and Mechanical Properties of (Ti, Al)(O, N) Films Synthesized by Reactive Sputtering, *Mater. Lett.*, 2006, **60**(3), p 375–378
5. J. Sjölén, L. Karlsson, S. Braun, R. Murdey, A. Hörling, and L. Hultman, Structure and Mechanical Properties of Arc Evaporated Ti–Al–O–N Thin Films, *Surf. Coat. Technol.*, 2007, **201**(14), p 6392–6403

6. B.E. Warren, X-Ray Studies of Deformed Metals, *Prog. Met. Phys.*, 1959, **9**, p 147–202
7. F. Vaz, J. Ferreira, E. Ribeiro, L. Rebouta, S. Lanceros-Méndez, J.A. Mendes, E. Alves, Ph. Goudeau, J.P. Riviére, F. Ribeiro, I. Moutinho, K. Pischow, and J. De Rijk, Influence of Nitrogen Content on the Structural, Mechanical and Electrical Properties of TiN Thin Films, *Surf. Coat. Technol.*, 2005, **191**(2–3), p 317–323
8. G.G. Stoney, The Tension of Metallic Films Deposited by Electrolysis, *Proc. R Soc. Lond. Ser. A*, 1909, **82**, p 172–175
9. H. Conrad, Effect of Grain Size on the Lower Yield and Flow Stress of Iron and Steel, *Acta Metall.*, 1963, **11**(1), p 75–77
10. H. Wang, A. Sharma, A. Kvit, X. Zhang, C.C. Koch, J. Narayan, and Q. Wei, Mechanical Properties of Nanocrystalline and Epitaxial TiN Films on (100) Silicon, *J. Mater. Res.*, 2001, **16**(9), p 2733–2738
11. H. Conrad and J. Narayan, On the Grain Size Softening in Nanocrystalline Materials, *Scripta Mater.*, 2000, **42**(11), p 1025–1030
12. J. Musil and J. Vlček, Magnetron Sputtering of Alloy-Based Films and its Specificity, *Czech J. Phys.*, 1998, **48**(10), p 1209–1224
13. S. Vepřek and S. Reiprich, A Concept for the Design of Novel Superhard Coatings, *Thin Solid Films*, 1995, **268**(1–2), p 64–71
14. R.W. Siegel, Nanophase Materials: Structure, Defects and Properties, *Proc. ATC Int. Symp. (ACTA)*, 1996, **1**, p 144–152
15. C.P. Constable, J. Yarwood, and W.-D. Münz, Raman Microscopic Studies of PVD Hard Coatings, *Surf. Coat. Technol.*, 1999, **116–119**, p 155–159
16. G.-R. Gu, Y.-A. Li, Y.-C. Tao, Z. He, J.-J. Li, H. Yin, W.-Q. Li, and Y.-N. Zhao, Investigation on the Structure of TiO_2 Films Sputtered on Alloy Substrates, *Vacuum*, 2003, **71**(4), p 487–490